Chapter 7

External Forced Convection

In this course, discussion is limited to low speed, forced convection, with no phase change within the fluid.

7.1 The Empirical Method
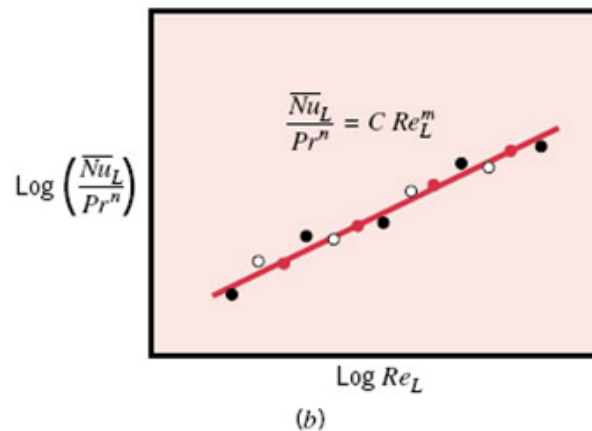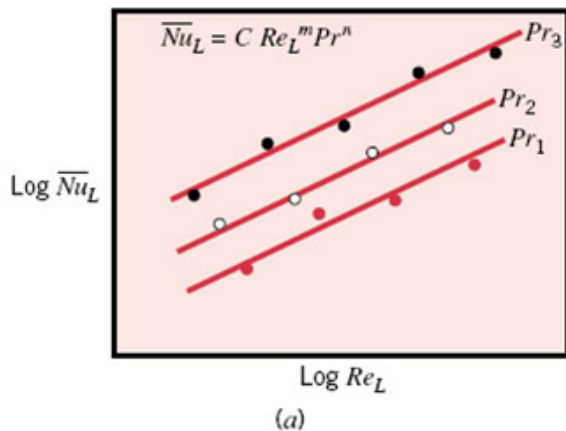
$$Nu_x = f(x^*, Re_x, Pr) \tag{6.49}$$

$$\overline{Nu}_x = f(Re_x, Pr) \tag{6.50}$$

The empirical correlation of the form

$$\overline{Nu}_L = CRe_L^m Pr^n \tag{7.1}$$

may be determined experimentally, as shown in Figs. 7.1-7.2.

for fixed Pr

$$\log \overline{Nu}_L = \log C + m \log Re_L$$

for fixed Re_L

$$\log \overline{Nu}_L = \log C + n \log Pr$$

FIGURE 7.2 Dimensionless representation of convection heat transfer measurements.

Heat transfer: $\overline{Nu}_L = CRe_L^m Pr^n$ (7.1)

Mass transfer: $\overline{Sh}_L = CRe_L^m Sc^n$ (7.3)

<u>Note</u>: To account for the effect of non-uniform temperature on fluid properties, there are two methods:

(1) To evaluate fluid properties at the *film temperature*

$$T_f \equiv \frac{T_s + T_\infty}{2}$$ (7.2)

(2) To evaluate all properties at and to correct with a parameter of the form $(Pr_\infty/Pr_s)^r$ or $(\mu_\infty/\mu_s)^r$.

7.2 The Flat Plate in Parallel Flow

7.2.1 Laminar Flow Over an Isothermal Plate: A Similarity Solution

Read the textbook pp. 405-410.

With stream function $\psi(x, y)$ and the transformation of $\eta, f(\eta)$ defined in (7.9), (7.10), the continuity equation (7.4) together with the steady-state momentum equation (7.5) can be reduced to a single ordinary differential equation (7.17), subjected to BCs (7.18). The numerical solution is shown in Table 7.1. The boundary layer thickness δ and the local friction coefficient $C_{f,x}$ can be determined as (7.19) and (7.20).

TABLE 7.1 Flat plate laminar boundary layer functions [3]

$\eta = y\sqrt{\dfrac{u_\infty}{vx}}$	f	$\dfrac{df}{d\eta} = \dfrac{u}{u_\infty}$	$\dfrac{d^2f}{d\eta^2}$
0	0	0	0.332
0.4	0.027	0.133	0.331
0.8	0.106	0.265	0.327
1.2	0.238	0.394	0.317
1.6	0.420	0.517	0.297
2.0	0.650	0.630	0.267
2.4	0.922	0.729	0.228
2.8	1.231	0.812	0.184
3.2	1.569	0.876	0.139
3.6	1.930	0.923	0.098
4.0	2.306	0.956	0.064
4.4	2.692	0.976	0.039
4.8	3.085	0.988	0.022
5.2	3.482	0.994	0.011
5.6	3.880	0.997	0.005
6.0	4.280	0.999	0.002
6.4	4.679	1.000	0.001
6.8	5.079	1.000	0.000

$$C_{f,x} \equiv \frac{\tau_{s,x}}{\rho u_\infty^2 / 2} = 0.664 Re_x^{-1/2} \qquad (7.20)$$

Similarly, the energy equation can be reduced to (7.21), subjected to BCs (7.22). Numerical integration leads to

$$\left. \frac{dT*}{d\eta} \right|_{\eta=0} = 0.332 Pr^{1/3}$$

and

$$Nu_x \equiv \frac{h_x x}{k} = 0.332 Re_x^{1/2} Pr^{1/3} \qquad Pr \geq 0.6 \qquad (7.23)$$

From the solution of (7.21), it also follows that $\quad \dfrac{\delta}{\delta_t} \approx Pr^{1/3} \qquad (7.24)$

The average heat transfer coefficient is

$$\overline{h}_x = \frac{1}{x} \int_0^x h_x dx = \ldots = 2h_x$$

Hence,

$$\overline{Nu}_x \equiv \frac{\overline{h}_x x}{k} = 0.664 Re_x^{1/2} Pr^{1/3} \qquad Pr \geq 0.6 \qquad (7.30)$$

Similarly,

$$\overline{Sh}_x \equiv \frac{\overline{h}_{m,x} x}{D_{AB}} = 0.664 Re_x^{1/2} Sc^{1/3} \qquad Sc \geq 0.6 \qquad (7.31)$$

- For small Pr, namely *liquid metals*, $\delta_t >> \delta$, we may assume $u=u_\infty$ throughout the thermal boundary layer and obtain (7.32).
- For all Pr numbers: (7.33)

7.2.2 Turbulent Flow over an Isothermal Plate

From experiment, it is known

$$C_{f,x} = 0.0592 Re_x^{-1/5} \qquad Re_x \le 10^7 \qquad (7.34)$$

Moreover,

$$\delta = 0.37 x Re_x^{-1/5} \qquad (7.35)$$

For turbulent flow,

$$\delta \approx \delta_t \approx \delta_c$$

Using (7.35) with the modified Reynolds analogy,

$$Nu_x = St\, Re_x Pr = 0.0296 Re_x^{4/5} Pr^{1/3} \qquad 0.6 < Pr < 60 \qquad (7.36)$$

$$Sh_x = St_m\, Re_x Sc = 0.0296 Re_x^{4/5} Sc^{1/3} \qquad 0.6 < Sc < 3000 \qquad (7.37)$$

- Enhanced mixing causes the turbulent boundary layer to grow more rapidly than the laminar boundary layer (δ varies as $x^{4/5}$ in contrast to $x^{1/2}$ for laminar flow) and to have larger friction and convection coefficients.

7.2.3 Mixed boundary Layer Conditions

When transition occurs sufficiently upstream of the trailing edge, $(x_c/L) \lesssim 0.95$ (Fig. 7.3), both the laminar and the boundary layers should be considered.
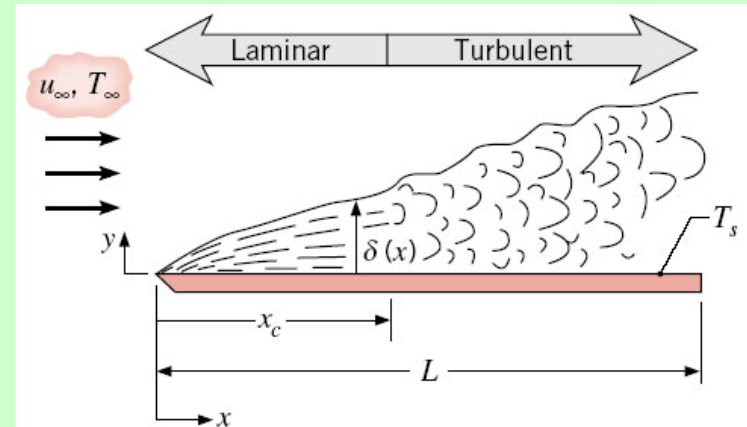
General expressions:

$$\overline{Nu}_L = (0.037 Re_L^{4/5} - A) Pr^{1/3} \quad \begin{bmatrix} 0.6 \leq Pr \leq 60 \\ Re_{x,c} \leq Re_L \leq 10^8 \end{bmatrix} \qquad (7.38)$$

$$A = 0.037 Re_{x,c}^{4/5} - 0.664 Re_{x,c}^{1/2} \qquad (7.39)$$

$$\overline{C}_{f,L} = 0.074 Re_L^{-1/5} - \frac{2A}{Re_L} \quad \begin{bmatrix} Re_{x,c} \leq Re_L \leq 10^8 \end{bmatrix} \qquad (7.40)$$

$$\overline{Sh}_L = (0.037 Re_L^{4/5} - A) Sc^{1/3} \quad \begin{bmatrix} 0.6 \leq Sc \leq 60 \\ Re_{x,c} \leq Re_L \leq 10^8 \end{bmatrix} \qquad (7.41)$$

7.2.4 Unheated Starting Length
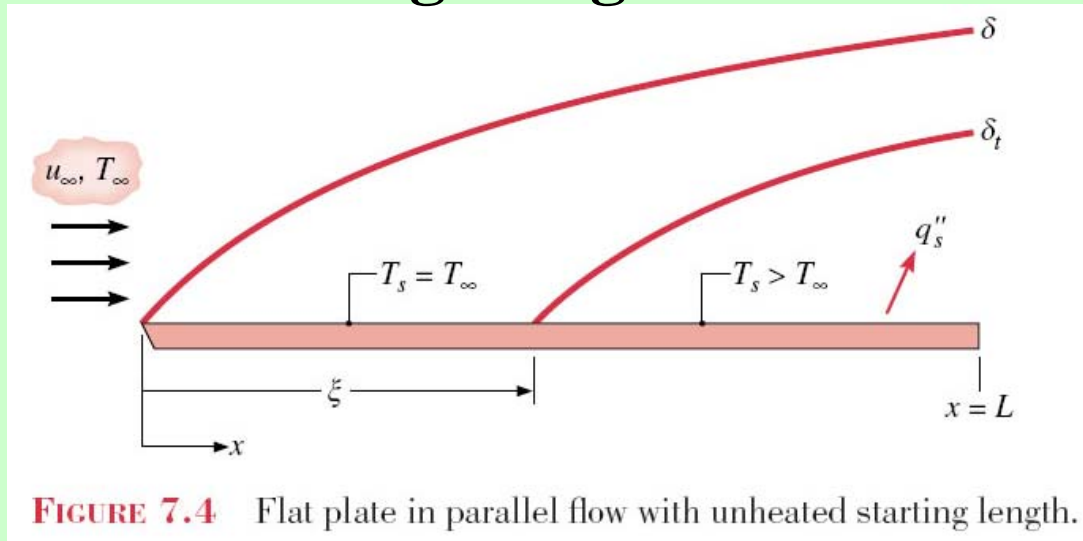
FIGURE 7.4 Flat plate in parallel flow with unheated starting length.

For flat plate in parallel flow with *unheated starting length* (Fig. 7.4):

Laminar flow:
$$Nu_x = \frac{Nu_x\big|_{\xi=0}}{\left[1-(\xi/x)^{3/4}\right]^{1/3}}$$
(7.42)

turbulent flow:
$$Nu_x = \frac{Nu_x\big|_{\xi=0}}{\left[1-(\xi/x)^{9/10}\right]^{1/9}}$$
(7.43)

7.2.5 Flat Plates with Constant Heat Flux Conditions

For flat plate with a *uniform surface heat flux*:

laminar flow: $Nu_x \equiv \dfrac{h_x x}{k} = 0.453 Re_x^{1/2} Pr^{1/3}$, $Pr \geq 0.6$ (7.45)

$\Leftrightarrow$ in comparison with (7.23)

turbulent flow: $Nu_x = St\, Re_x Pr = 0.0308 Re_x^{4/5} Pr^{1/3}$, $0.6 < Pr < 60$ (7.46)

$\Leftrightarrow$ in comparison with (7.36)

In this case, $T_s(x) = T_\infty + \dfrac{q_s''}{h_x}$ is varying. The local surface temperature is

$$\overline{(T_s - T_\infty)} = \frac{1}{L} \int_0^L (T_s - T_\infty)\, dx = \frac{q_s''}{L} \int_0^L \frac{x}{k Nu_x}\, dx \qquad (7.48)$$

$$= \frac{q_s'' L}{k \overline{Nu}_L}$$

where $\overline{Nu}_L = 0.680 Re_L^{1/2} Pr^{1/3}$ (7.49)

Note: Any of the $\overline{Nu}_L$ results obtained for a uniform surface temperature may be used with Eq. 7.48 to evaluate $(T_s - T_\infty)$.

7.2.6 Limitations on Use of Convection Coefficients

Errors as large as 25% may be incurred by using the expressions due to varying free stream turbulence and surface roughness.

7.3 Methodology for a Convection Calculation

Follow the six steps listed in the textbook.

1. Become immediately cognizant of the flow geometry.

2. Specify the appropriate reference temperature and evaluate the pertinent fluid properties at that temperature.

3. In mass transfer problems the pertinent fluid properties are those of species B.

4. Calculate the Reynolds number.

5. Decide whether a local or surface average coefficient is required.

6. Select the appropriate correlation.

EXs 7.1-7.3

7.4 The Cylinder in Cross Flow

Boundary layer *separation* may occur due to the adverse pressure gradient ($dp/dx > 0$). Boundary layer transition, from laminar b. l. to turbulent b. l., depends on Re_D ($\equiv \rho VD/\mu$).
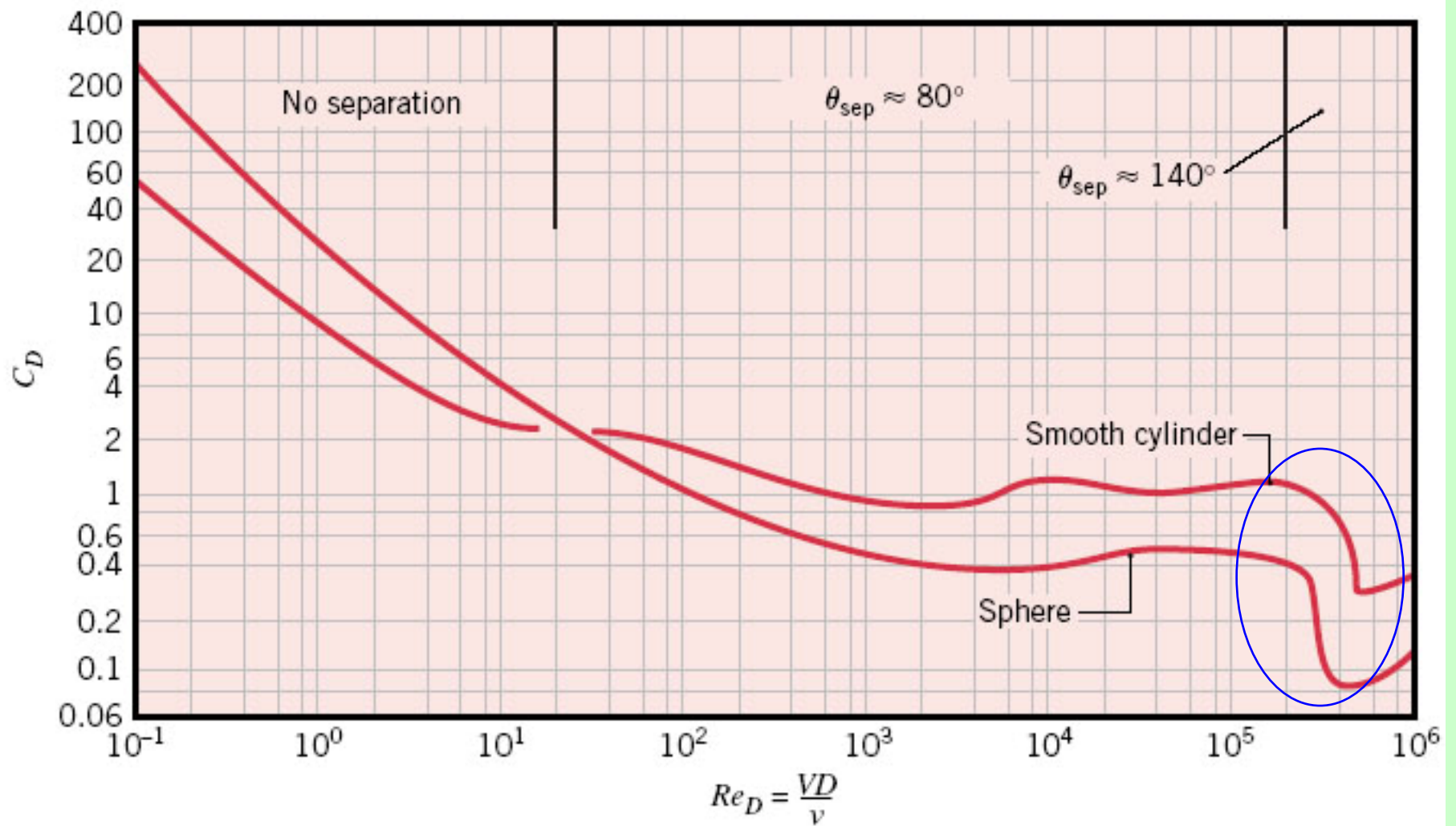
Drag coeff. $C_D \rightarrow$ Fig. 7.8
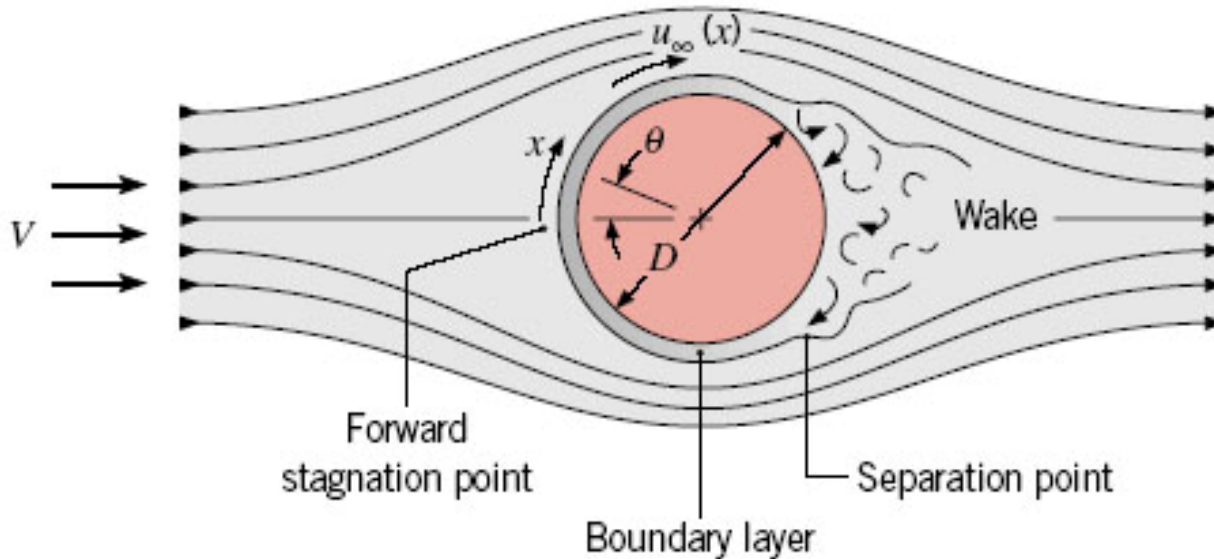
FIGURE 7.5 Boundary layer formation and separation on a circular cylinder in cross flow.

Favorable pressure gradient | Adverse pressure gradient

$$\frac{\partial p}{\partial x} < 0 \qquad\qquad \frac{\partial p}{\partial x} > 0$$

$u_\infty(x)$

Separation point

Flow reversal

Wake

Vortices
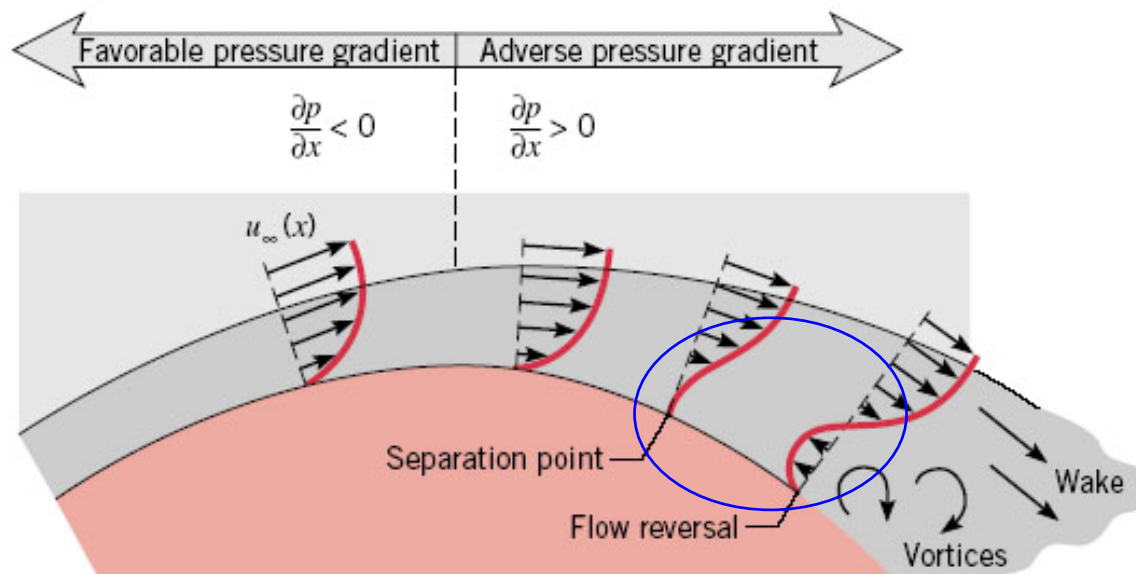
FIGURE 7.6 Velocity profile associated with separation on a circular cylinder in cross flow.

Laminar boundary layer

θ_{sep}

V

$Re_D \lesssim 2 \times 10^5$

Separation

Laminar boundary layer

Transition

Turbulent boundary layer

θ_{sep}

V

$Re_D \gtrsim 2 \times 10^5$
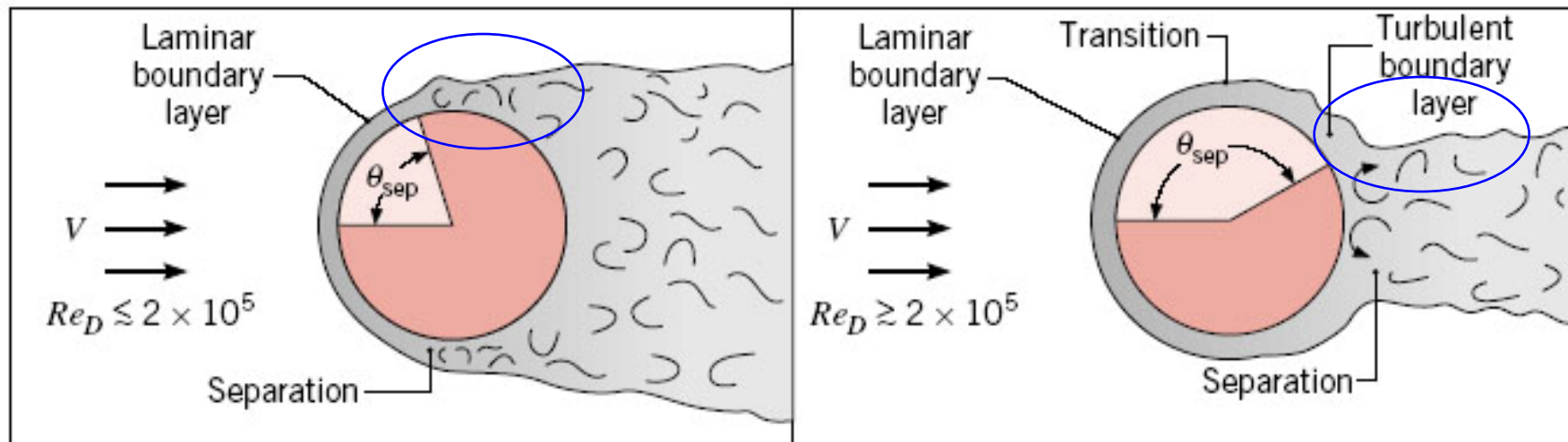
Separation

FIGURE 7.7 The effect of turbulence on separation.

No separation

$\theta_{sep} \approx 80°$

$\theta_{sep} \approx 140°$

Smooth cylinder

Sphere

C_D

$Re_D = \dfrac{VD}{v}$

FIGURE 7.8 Drag coefficients for a smooth circular cylinder in cross flow and for a sphere [2]. Boundary layer separation angles are for a cylinder. Adapted with permission.

7.4.2 Convection Heat and Mass Transfer

The local $Nu_\theta \rightarrow$ Fig. 7.9

Rise due to transition to turbulence
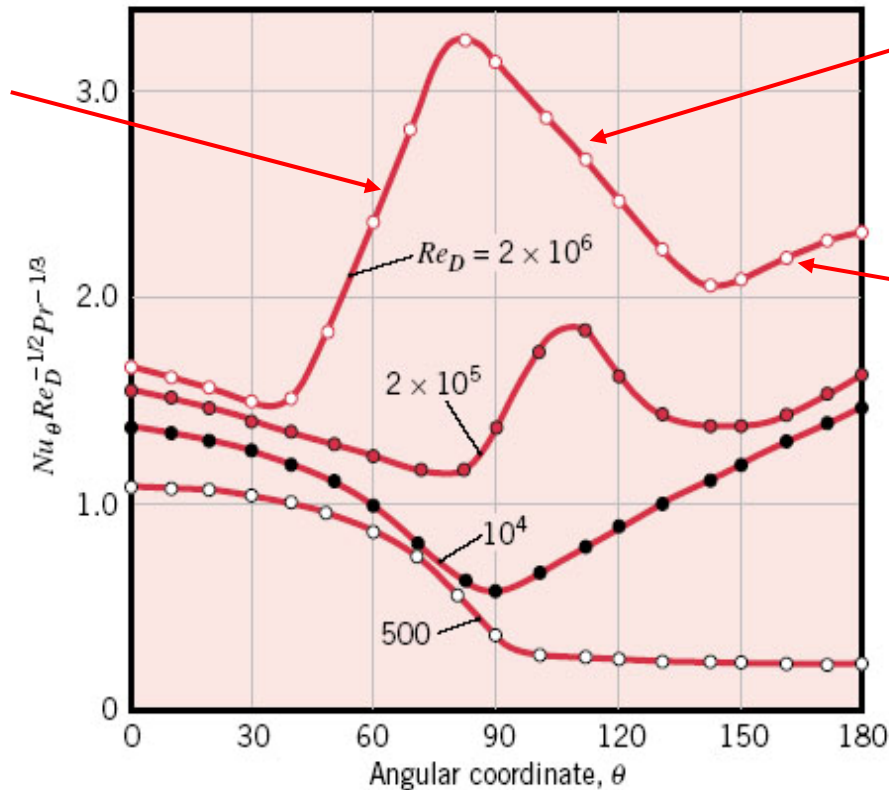
Decline due boundary layer growth

Rise due to mixing in the wake

FIGURE 7.9 Local Nusselt number for airflow normal to a circular cylinder. Adapted with permission from Zukauskas, A., "Convective Heat Transfer in Cross Flow," in S. Kakac, R. K. Shah, and W. Aung, Eds., *Handbook of Single-Phase Convective Heat Transfer*, Wiley, New York, 1987.

The average (of more engineering interest):

$$\overline{Nu_D} \equiv \frac{\overline{h}D}{k} = C Re_D^m Pr^{1/3} \qquad \text{--empirical} \qquad (7.52)$$

Constants for circular cylinders: Table 7.2
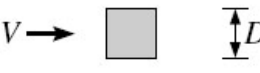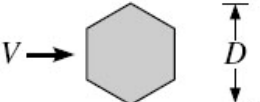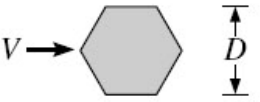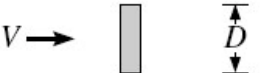
TABLE 7.2 Constants of Equation 7.52 for the circular cylinder in cross flow [11, 12]

Re_D	C	m
0.4–4	0.989	0.330
4–40	0.911	0.385
40–4000	0.683	0.466
4000–40,000	0.193	0.618
40,000–400,000	0.027	0.805

$$\overline{Nu}_D \equiv \frac{\overline{h}D}{k} = CRe_D^m Pr^{1/3} \qquad (7.52)$$

Constants for noncircular cylinders: Table 7.3

TABLE 7.3 Constants of Equation 7.52 for noncircular cylinders in cross flow of a gas [13]

Geometry	Re_D	C	m
Square			
$V \to$ ◇ D	$5 \times 10^3 - 10^5$	0.246	0.588
$V \to$ ◻ D	$5 \times 10^3 - 10^5$	0.102	0.675
Hexagon			
$V \to$ ⬡ D	$5 \times 10^3 - 1.95 \times 10^4$	0.160	0.638
	$1.95 \times 10^4 - 10^5$	0.0385	0.782
$V \to$ ⬡ D	$5 \times 10^3 - 10^5$	0.153	0.638
Vertical plate			
$V \to$ ▯ D	$4 \times 10^3 - 1.5 \times 10^4$	0.228	0.731

Other correlations are shown in (7.53), (7.54).

EX 7.4

7.5 The Sphere

Whitaker:

$$\overline{Nu}_D = 2 + (0.4 Re_D^{1/2} + 0.06 Re_D^{2/3}) Pr^{0.4} \left(\frac{\mu}{\mu_s} \right)^{1/4} \qquad (7.56)$$

$$\begin{bmatrix} 0.71 \leq Pr \leq 380 \\ 3.5 \leq Re_D \leq 7.6 \times 10^4 \\ 1.0 \leq (\mu / \mu_s) \leq 3.2 \end{bmatrix}$$

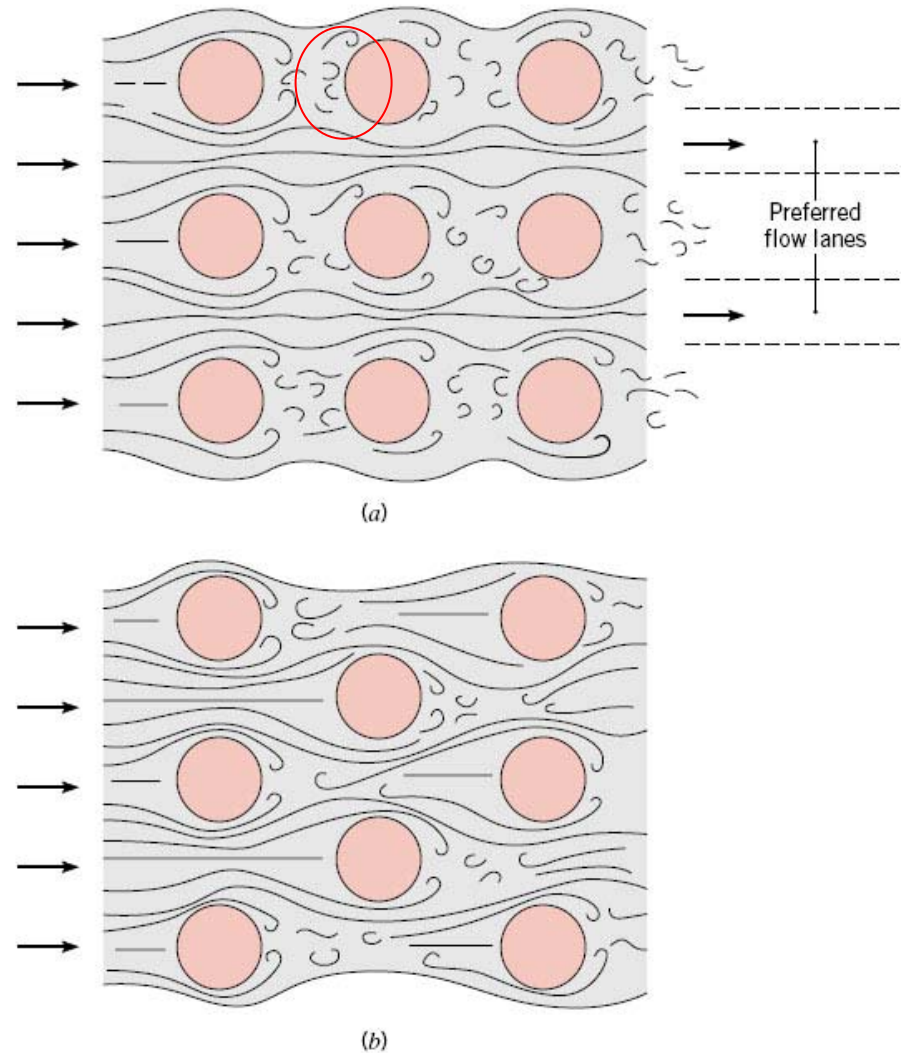- For liquid drops the Ranz and Marshall correlation (7.57). More accurate modifications for it are also available.

$$\overline{Nu}_D = 2 + 0.6 Re_D^{1/2} Pr^{1/3} \qquad (7.57)$$

EX 7.6

7.6 Flow across Banks of Tubes (brief introduction)
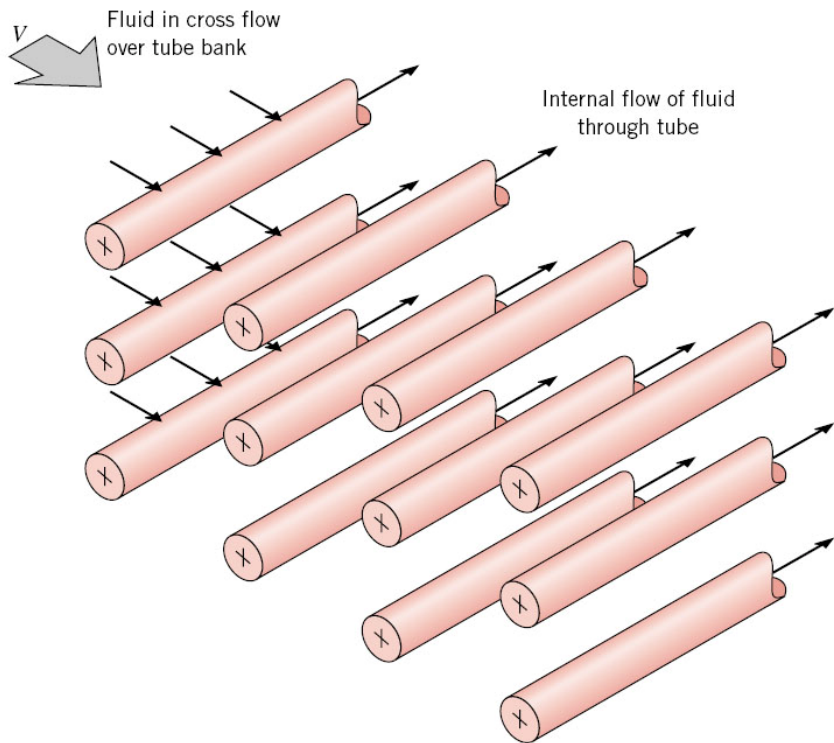
FIGURE 7.10 Schematic of a tube bank in cross flow.

V

Fluid in cross flow over tube bank

Internal flow of fluid through tube

(a)

Preferred flow lanes

(b)

FIGURE 7.12 Flow conditions for (a) aligned and (b) staggered tubes.

- Aligned or staggered: Fig. 7.11 and Fig. 7.12
- A number of correlations for $\overline{Nu}_D$ are given in (7.58)-(7.65), with constants listed in Tables 7.5-7.8.
- The *h* for a tube in the first row is approximately equal to that for a single tube in cross flow, whereas larger heat transfer coefficients are associated with tubes of the inner rows. Mostly, the convection coefficient stabilizes for a tube beyond the fourth or fifth row.
- In general, heat transfer enhancement is favored by the more tortuous flow of a staggered arrangement, particularly for small Re_D (<100).
- Since the fluid temperature may change over the tube bank, the heat transfer rate may be significantly over-predicted by using $\Delta T = T_s - T_\infty$. The appropriate form of ΔT is a *log-mean temperature difference* ΔT_{lm}, as shown in (7.66). And

$$q' = N(\overline{h}\,\pi D \Delta T_{lm}) \qquad (7.68)$$

- The pressure drop (7.69)

7.7 Impinging Jets (brief introduction)

The impinging jet is a simple and effective way of cooling. The compressed boundary layer near the central stagnation point causes effective cooling of the surface. It is widely adopted, in combination of cooling fins, in CPU cooling for desktop PCs and other types of computers.
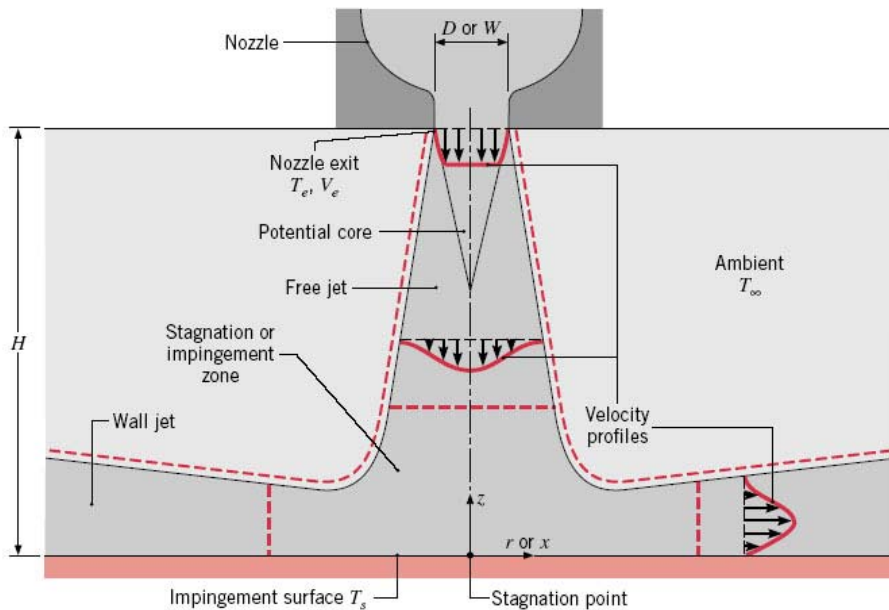
FIGURE 7.15 Surface impingement of a single round or slot gas jet.
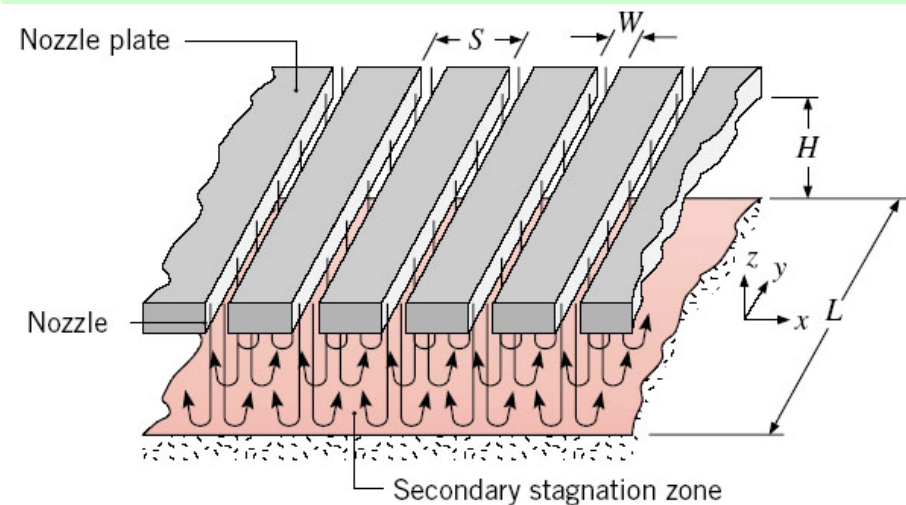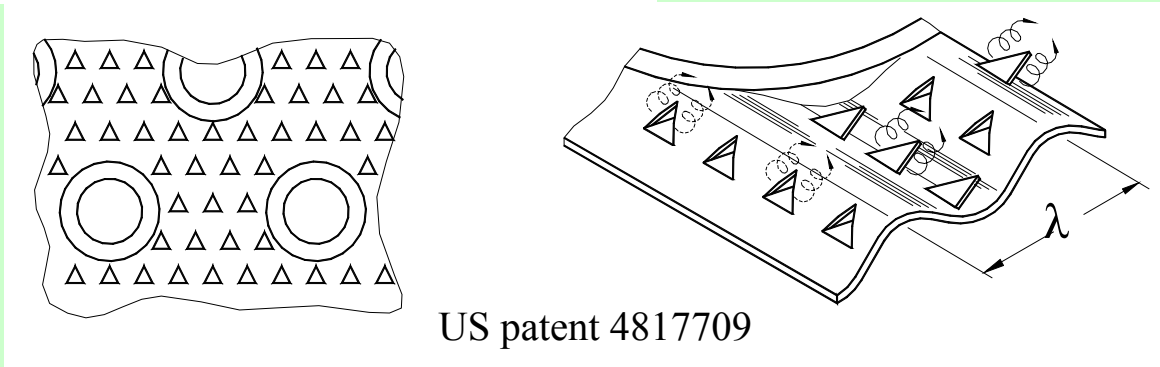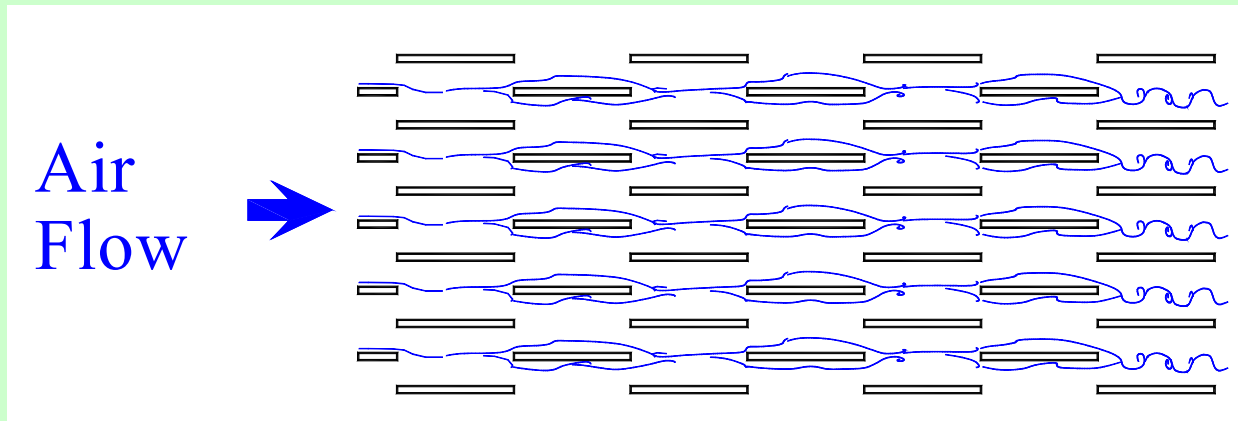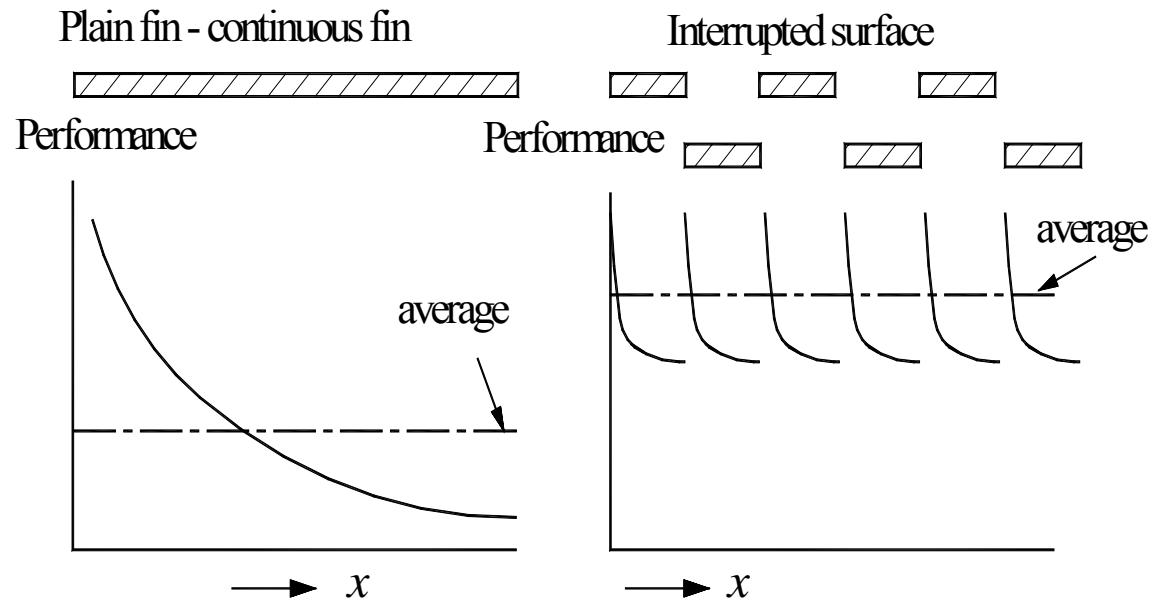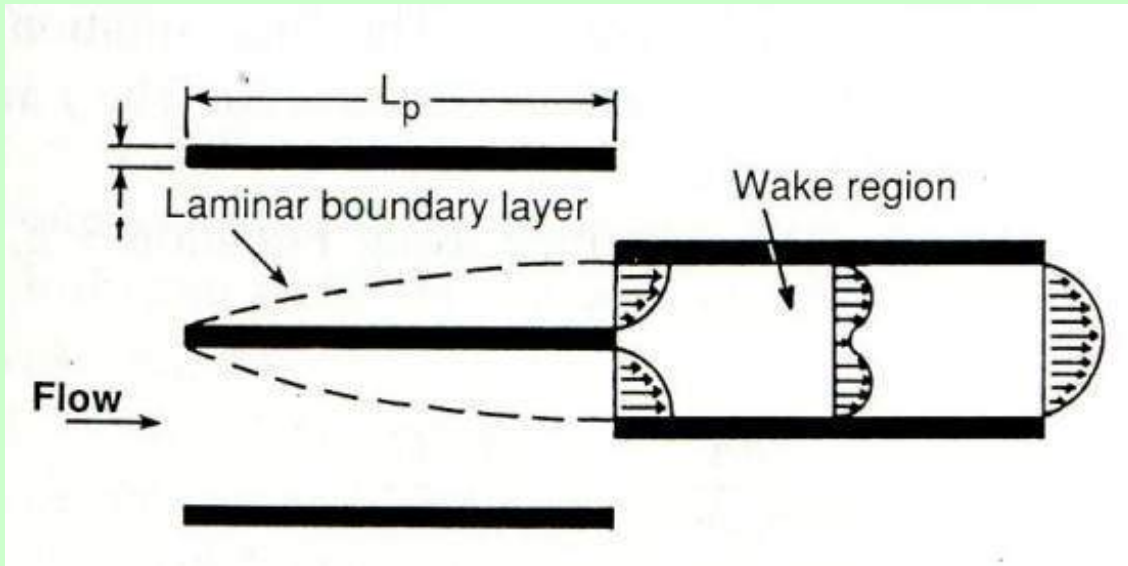

FIGURE 7.16 Surface impingement of an array of slot jets.

Heat Transfer Enhancement

- Boundary layer regrowth
- Flow transition or turbulence
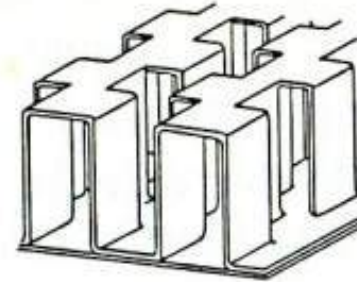
Air Flow

US patent 4817709

Heat Transfer Enhancement
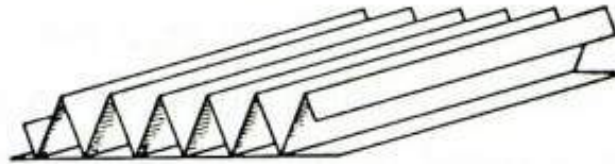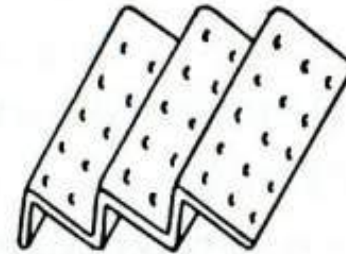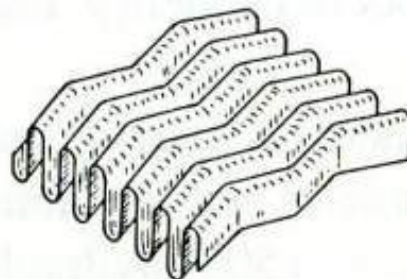
Heat Transfer Enhancement

a. Rectangular
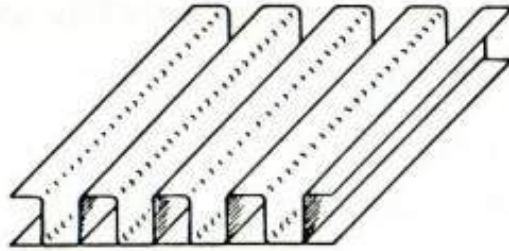
d. Offset Strip Fin

b. Triangular

e. Perforated

c. Wavy

f. Louvered